

Interaction of water with (silico)aluminophosphate zeotypes: A comparative investigation using dispersion-corrected DFT

Michael Fischer

Fachgebiet Kristallographie, Fachbereich Geowissenschaften, Universität Bremen,
Klagenfurter Straße, 28359 Bremen, Germany

and

MAPEX Center for Materials and Processes, Universität Bremen, Germany

michael.fischer@uni-bremen.de

ELECTRONIC SUPPLEMENTARY INFORMATION

- 1) DFT-D optimisations of guest-free AlPO and SAPO models**
- 2) DFT-D results: AlPOs with large amounts of adsorbed water**
- 3) DFT-D results: SAPOs with small amounts of adsorbed water**
- 4) DFT-D results: SAPOs with large amounts of adsorbed water**

1) DFT-D optimisations of guest-free AIPO and SAPO models

1.1 Optimised lattice parameters of AIPO models

Table S1: DFT-D optimised lattice parameters of guest-free AIPO structures. For AIPO-18 and AIPO-RHO, the lattice parameters of the primitive cells are given to facilitate the comparison with the values for SAPOs reported below.

	FTC	Space group	$a / \text{\AA}$	$b / \text{\AA}$	$c / \text{\AA}$	α / deg	β / deg	γ / deg	$V / \text{\AA}^3$
AIPO-34	CHA	$R-3$	13.792	$= a$	14.972	90	$= \alpha$	120	2466.4
AIPO-17	ERI	$P6_3/m$	13.205	$= a$	15.385	90	$= \alpha$	120	2323.2
AIPO-AFX	AFX	$P-31c$	13.774	$= a$	20.048	90	$= \alpha$	120	3293.8
AIPO-GIS	GIS	$Fddd$	13.979	13.778	10.349	90	$= \alpha$	$= \alpha$	1993.3
AIPO-18	AEI	$C2/c$	9.407	9.407	18.649	89.87	$= \alpha$	85.63	1645.5
AIPO-RHO	RHO	$I23$	13.097	$= a$	$= a$	109.47	$= \alpha$	$= \alpha$	1729.5

1.2 Detailed description and visualisation of SAPO models

In the following, the SAPO models considered in the DFT-D calculations for guest-free systems are described and visualised. The results of the calculations for the individual systems (lattice parameters and energy differences with respect to energetically most favourable models) are summarised in 1.3.

SAPO-34

As all phosphorus sites in the CHA framework are equivalent by symmetry, only one type of Si substitution was considered. In line with previous work,¹ the structure model of SAPO-34 has $P3_2$ symmetry (three Si atoms per hexagonal unit cell: $\text{Si}/(\text{Al}+\text{P}+\text{Si}) = 0.083$). In that study, it was already found that an attachment of H to the O1 oxygen atom (equatorial position of d6R unit) is the energetically most favourable scenario. Therefore, all calculations reported in the present work used the SAPO-34_O1 structure.

SAPO-34_O1

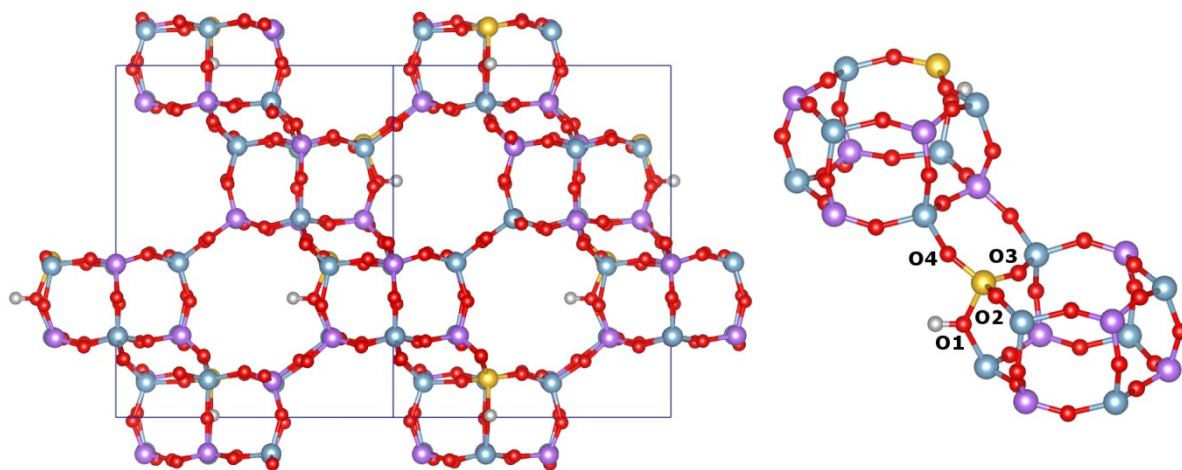
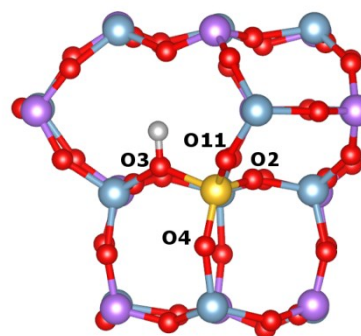
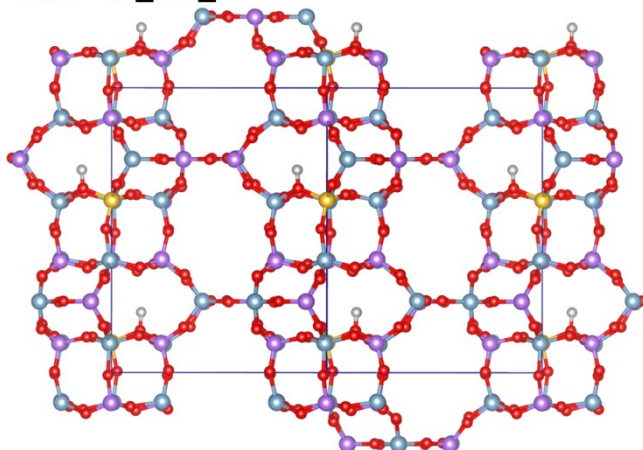


Figure S1: Enumeration of oxygen positions in SAPO-34. The proton position that is visualised corresponds to the energetically preferred location.

SAPO-17

There are two different T sites in the ERI framework: While T1 atoms form the six-rings that join the *d6r* units and cancrinite (*can*) cages, the T2 atoms are located in equatorial positions of the *can* cages. A solid-state NMR study of SAPO-17 provided evidence for a preferential incorporation of Si at the T2 site.² In the present study, both possible locations of Si were considered, introducing two Si atoms per unit cell ($\text{Si}/(\text{Al}+\text{P}+\text{Si}) = 0.056$). The symmetry was reduced to $P2_1$, with the *b*-axis of the monoclinic cell corresponding to the *c*-axis of the hexagonal AlPO-17 structure. Appropriate constraints were employed to retain a hexagonal cell shape. In the calculations considering different proton locations, SAPO-17_Si1_O3 (proton pointing across distorted six-ring window of *can* cage) and SAPO-17_Si2_O5 (proton pointing across single six-ring) were found to be the energetically preferred situations. As both systems are very close in energy (within 2 kJ mol^{-1}), the DFT-D calculations provide no evidence for a thermodynamic preference of silicon to occupy the T2 sites. However, such a preference could be caused by the structure-directing influence of template molecules.

SAPO-17_Si1_O3



SAPO-17_Si2_O5

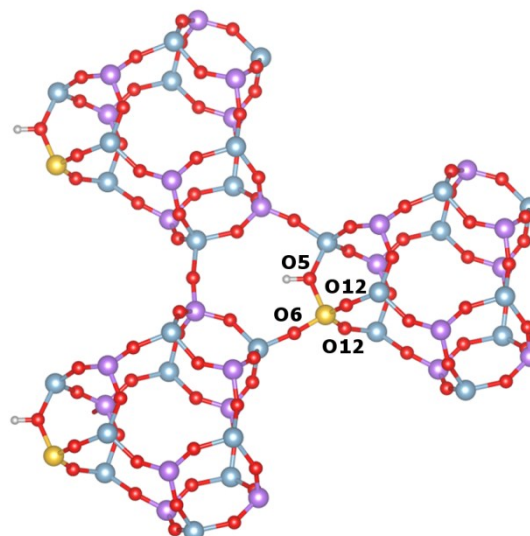
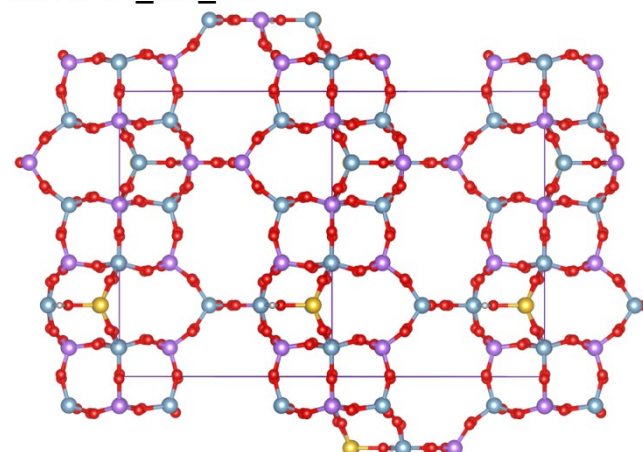
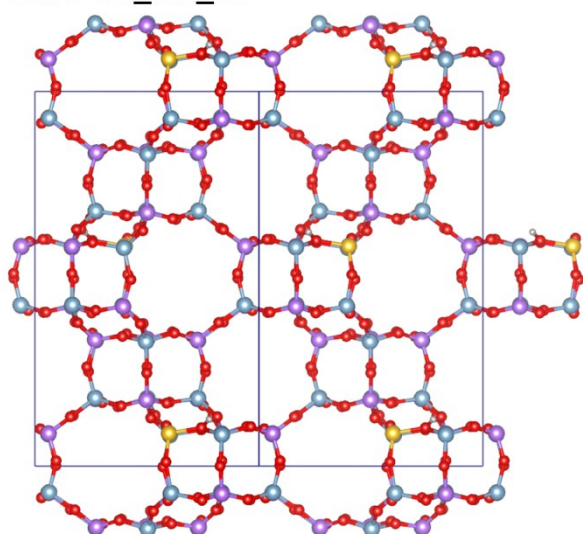


Figure S2: Enumeration of oxygen positions in SAPO-17. The proton positions that are visualised correspond to the energetically preferred locations.

SAPO-56

There are two non-equivalent T sites in the AFX framework: The T1 atoms are located in those $d6r$ units that constitute the top and bottom of the large aft cages, whereas the T2 atoms are part of the second type of $d6r$ units, which are located at the top and bottom of the smaller gmelinite (gme) cages. Two Si atoms per unit cell were introduced ($\text{Si}/(\text{Al}+\text{P}+\text{Si}) = 0.042$), and the symmetry was reduced to Bn (non-standard setting of Cc , with this choice of space group setting the primitive cell corresponds to the original cell of AlPO-AFX). Constraints were used to retain the hexagonal cell shape. The energetically preferred proton positions were found to be SAPO-56_Si1_O5 (proton at equatorial oxygen atom of $d6r$ unit) and SAPO-56_Si2_O4 (proton pointing across the six ring of $d6r$ unit).

SAPO-56_Si1_O5



SAPO-56_Si2_O4

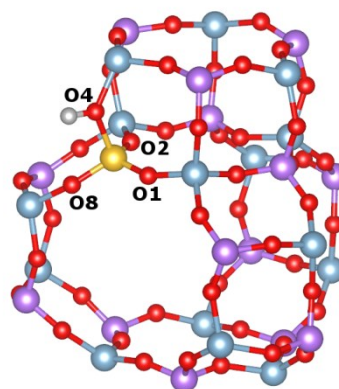
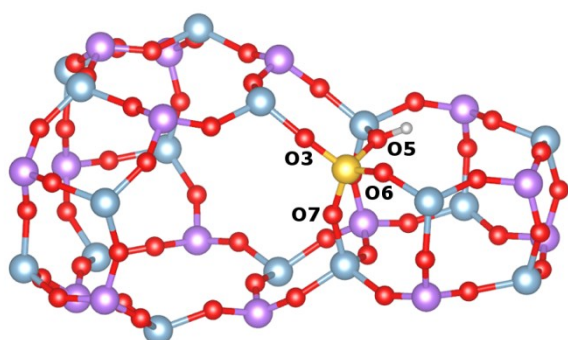
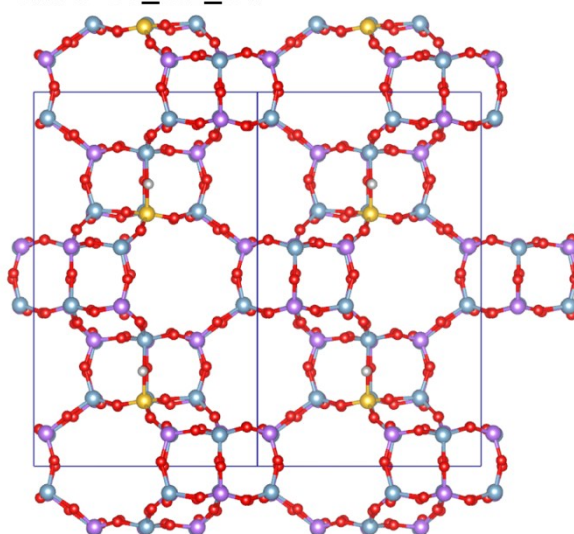


Figure S3: Enumeration of oxygen positions in SAPO-56. The proton positions that are visualised correspond to the energetically preferred locations.

SAPO-43

There is only one type of T site in the GIS framework. To build a model of SAPO-43, two Si atoms were placed in the unit cell ($\text{Si}/(\text{Al}+\text{P}+\text{Si}) = 0.063$), reducing the symmetry to $P-1$. The cell angles were constrained to 90 degrees in order to retain the orthorhombic cell shape. While three of the four possible locations of the framework proton are virtually identical in energy, only the most favourable system (SAPO-43_O12) was considered in the calculations including guest molecules. Compared to the other possible arrangements, the proton-proton distances are particularly large in this model ($\sim 10 \text{ \AA}$).

SAPO-43_O12

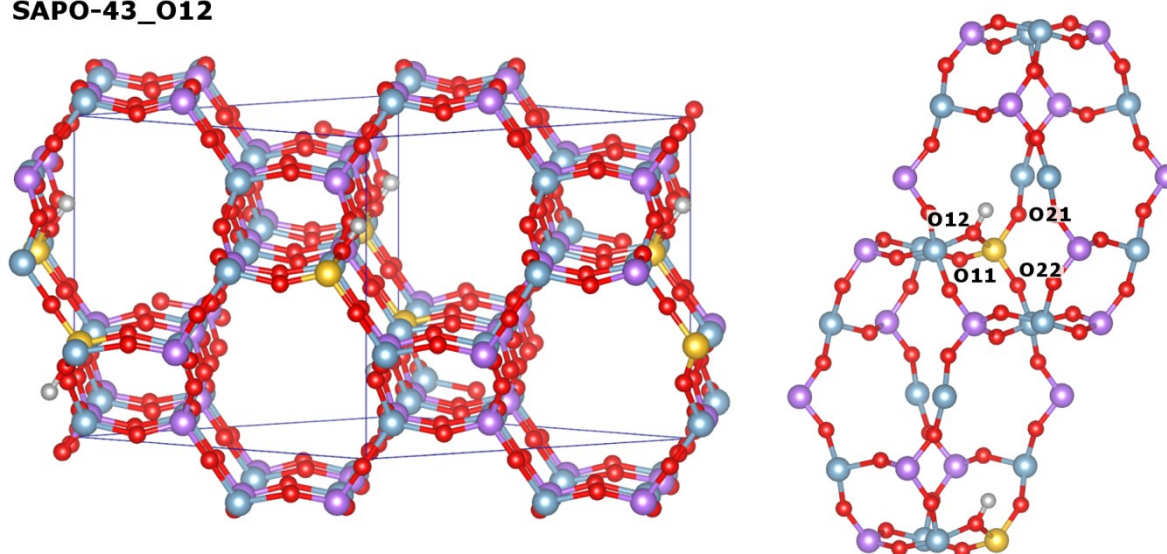


Figure S4: Enumeration of oxygen positions in SAPO-43. The proton position that is visualised corresponds to the energetically preferred location.

SAPO-18

For SAPO-18, a structure model in space group Cn (non-standard setting of Cc) was used, as the primitive cell of the structure in this setting is particularly convenient for the calculations (with all angles being close to 90 degrees). Two Si atoms were placed in the primitive unit cell ($\text{Si}/(\text{Al}+\text{P}+\text{Si}) = 0.083$). As there are three distinct T sites in the AEI framework, a total of twelve SAPO-18_SiX_OY models were considered. The energetically preferred situations are SAPO-18_Si1_O12 and SAPO-18_Si2_O11, which are very close in energy, and SAPO-18_Si3_O31, with the last system being 3.5 kJ mol^{-1} per proton less favourable than SAPO-18_Si2_O11. In the former two systems, the proton is attached to an equatorial oxygen atom of the $d6r$ units (like in SAPO-34_O1), whereas the proton points into the six-ring in SAPO-34_Si3_O31.

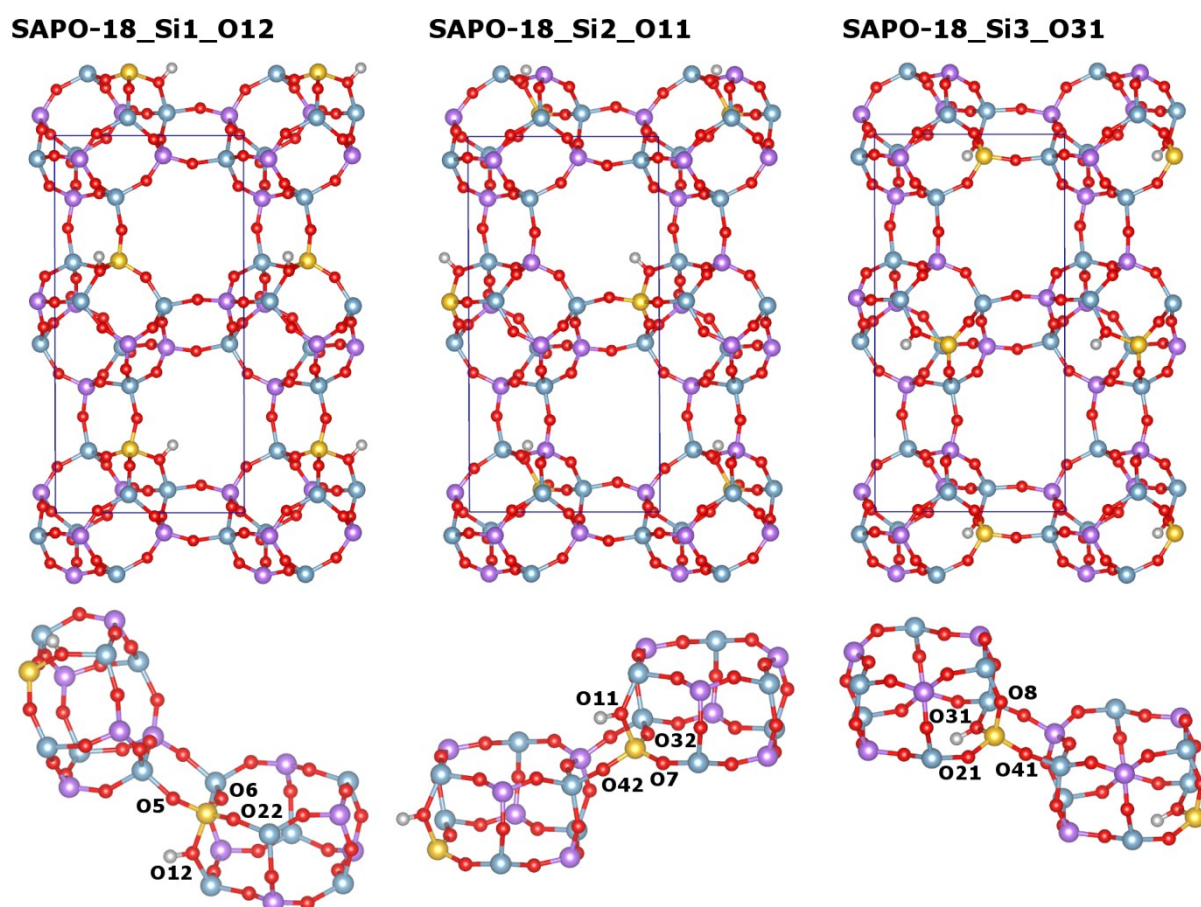


Figure S5: Enumeration of oxygen positions in SAPO-18. The proton positions that are visualised correspond to the energetically preferred locations.

SAPO-RHO

For SAPO-RHO, the primitive cell of the body-centered cubic unit cell of AlPO-RHO was used, and two Si atoms were placed in this unit cell ($\text{Si}/(\text{Al}+\text{P}+\text{Si}) = 0.083$). The symmetry of this model is $I2$ (non-standard setting of $C2$). In order to retain the cubic cell shape, the lattice parameters a , b , and c were constrained to having the same value, and the angles were constrained to 109.47 degrees. Since all phosphorus sites are equivalent, only one possible arrangement of silicon atoms in the framework was considered. In this system, there are no Si atoms sharing a common six-ring or four-ring, arrangements that are likely to be energetically unfavourable. In the energetically preferred model, SAPO-RHO_O11, two protons are located inside the eight-ring windows of one $d8r$ unit, pointing across the window.

SAPO-RHO_O11

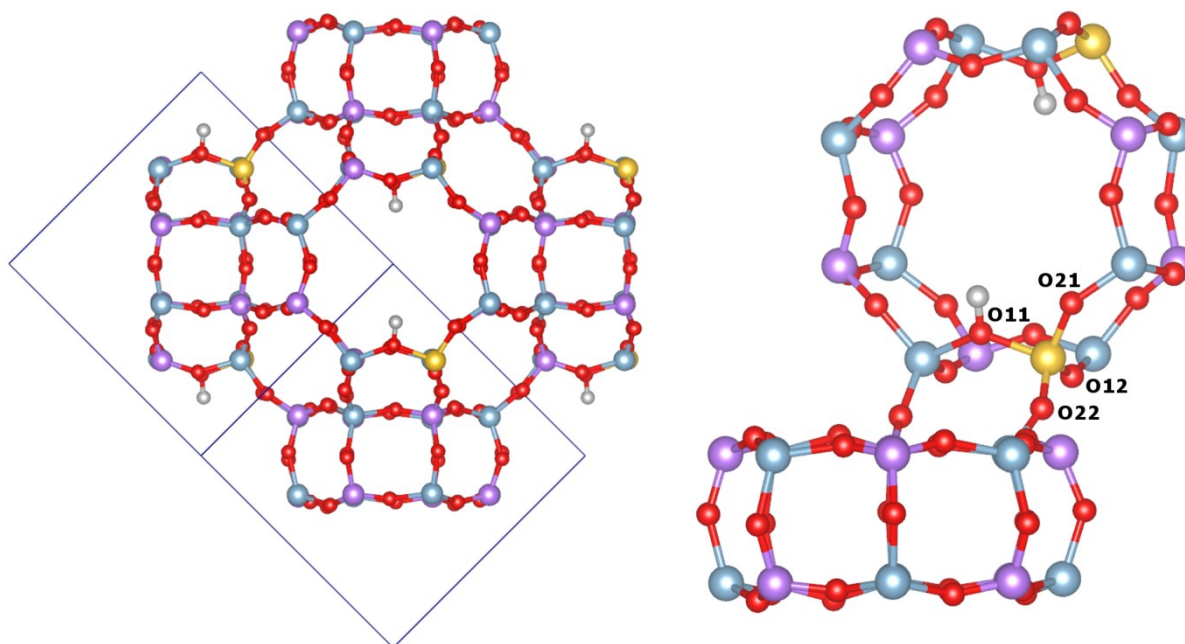


Figure S6: Enumeration of oxygen positions in SAPO-RHO. The proton position that is visualised corresponds to the energetically preferred location.

1.3 Optimised lattice parameters of SAPO models

Table S2: DFT-D optimised lattice parameters of SAPO-34. As discussed above, only the proton position at O1 was considered in the present study.

	$a / \text{Å}$	$c / \text{Å}$	$V / \text{Å}^3$
SAPO-34_O1	13.804	15.156	2501.1

Table S3: DFT-D optimised lattice parameters of SAPO-17. In the model, the b -axis of the monoclinic cell corresponds to the c -axis of the hexagonal cell of AlPO-17. The energy difference (per proton) with respect to the most favourable system SAPO-17_Si1_O3 is also given. For each of the two Si sites, the system with the energetically preferred proton location is highlighted in bold.

	$a / \text{Å}$	$b / \text{Å}$	$V / \text{Å}^3$	$\Delta E / \text{kJ mol}^{-1}$
SAPO-17_Si1_O11	13.255	15.316	2330.6	3.9
SAPO-17_Si1_O2	13.254	15.296	2327.1	2.2
SAPO-17_Si1_O3	13.282	15.197	2321.7	0
SAPO-17_Si1_O4	13.231	15.403	2335.1	5.3
SAPO-17_Si2_O12	13.297	15.336	2348.2	5.4
SAPO-17_Si2_O5	13.265	15.412	2348.4	2.0
SAPO-17_Si2_O6	13.236	15.420	2339.7	21.6

Table S4: DFT-D optimised lattice parameters of SAPO-56. The cell axes of the primitive cell of the model with space group symmetry Bn coincide with the hexagonal axis system of AlPO-AFX. The energy difference (per proton) with respect to the most favourable system SAPO-56_Si2_O4 is also given. For each of the two Si sites, the system with the energetically preferred proton location is highlighted in bold.

	$a / \text{Å}$	$c / \text{Å}$	$V / \text{Å}^3$	$\Delta E / \text{kJ mol}^{-1}$
SAPO-56_Si1_O3	13.827	19.979	3307.9	7.4
SAPO-56_Si1_O5	13.822	20.034	3314.9	2.5
SAPO-56_Si1_O6	13.830	19.982	3310.0	5.5
SAPO-56_Si1_O7	13.818	20.058	3316.5	2.8
SAPO-56_Si2_O1	13.815	20.020	3309.2	3.5
SAPO-56_Si2_O2	13.837	19.970	3311.3	1.5
SAPO-56_Si2_O4	13.816	20.044	3313.6	0
SAPO-56_Si2_O8	13.833	19.957	3307.3	7.0

Table S5: DFT-D optimised lattice parameters of SAPO-43. The energy difference (per proton) with respect to the most favourable system SAPO-43_O12 is also given.

	$a / \text{Å}$	$b / \text{Å}$	$c / \text{Å}$	$V / \text{Å}^3$	$\Delta E / \text{kJ mol}^{-1}$
SAPO-43_O11	14.103	13.901	10.326	2024.3	0.1
SAPO-43_O12	14.096	13.888	10.336	2023.4	0
SAPO-43_O21	14.066	13.784	10.362	2009.0	0.1
SAPO-43_O22	14.048	13.853	10.350	2014.2	3.4

Table S6: DFT-D optimised lattice parameters of SAPO-18. The space group symmetry of the model is Cc , however, for reasons of efficiency, the primitive cell of the non-conventional setting Cn was used in the calculations. The parameters reported below refer to this cell. In this cell setting, $a = b \neq c$, and $\alpha = \beta \neq \gamma$. The energy difference (per proton) with respect to the most favourable system SAPO-18_Si2_O11 is also given. For each of the three Si sites, the system with the energetically preferred proton location is highlighted in bold.

	$a / \text{\AA}$	$c / \text{\AA}$	α / deg	γ / deg	$V / \text{\AA}^3$	$\Delta E / \text{kJ mol}^{-1}$
SAPO-18_Si1_O12	9.435	18.811	90.14	86.24	1670.9	1.1
SAPO-18_Si1_O22	9.421	18.802	90.16	85.81	1664.3	5.1
SAPO-18_Si1_O5	9.431	18.777	90.54	86.02	1666.1	8.7
SAPO-18_Si1_O6	9.448	18.758	90.53	85.45	1668.9	3.8
SAPO-18_Si2_O11	9.476	18.634	90.26	85.27	1667.4	0
SAPO-18_Si2_O32	9.464	18.695	89.62	85.45	1669.1	2.7
SAPO-18_Si2_O42	9.455	18.661	89.66	84.22	1659.8	6.5
SAPO-18_Si2_O7	9.443	18.710	90.10	85.50	1663.2	4.1
SAPO-18_Si3_O21	9.463	18.643	90.05	85.75	1665.1	4.9
SAPO-18_Si3_O31	9.447	18.728	90.08	86.10	1667.4	3.5
SAPO-18_Si3_O41	9.444	18.615	89.50	85.94	1656.0	6.6
SAPO-18_Si3_O8	9.448	18.761	89.90	85.95	1670.4	3.8

Table S7: DFT-D optimised lattice parameters of SAPO-RHO. The parameters reported below refer to the primitive cell of the model in space group $I2$. In this cell setting, $a = b = c$, and $\alpha = \beta = \gamma = 109.47 \text{ deg}$. The energy difference (per proton) with respect to the most favourable system SAPO-RHO_O12 is also given.

	$a / \text{\AA}$	$V / \text{\AA}^3$	$\Delta E / \text{kJ mol}^{-1}$
SAPO-RHO_O11	13.159	1754.3	0
SAPO-RHO_O12	13.159	1754.0	1.0
SAPO-RHO_O21	13.137	1745.1	5.3
SAPO-RHO_O22	13.143	1747.8	6.6

2) DFT-D results: AlPOs with large amounts of adsorbed water

The following tables report the interaction energies and lattice parameters of the DFT-D optimised snapshots of AlPOs with large amounts of adsorbed water (near saturation).

E_{int} Total interaction energy per water molecule (in kJ mol⁻¹)

$E_{int,nodisp}$ Non-dispersive contribution to interaction energy per water molecule (in kJ mol⁻¹)

$N(\text{Al}^{\text{V}})$ Number of five-coordinated Al atoms per unit cell

Table S8: AlPO-34 with 40 water molecules per unit cell

	E_{int}	$E_{int,nodisp}$	$a / \text{\AA}$	$b / \text{\AA}$	$c / \text{\AA}$	α / deg	β / deg	γ / deg	$V / \text{\AA}^3$	$N(\text{Al}^{\text{V}})$
#1	-65.8	-41.5	13.835	13.794	14.981	90.84	89.97	120.79	2455.5	0
#2	-64.7	-40.0	13.730	13.695	15.081	90.24	90.19	120.09	2453.5	0
#3	-64.8	-40.4	13.688	13.668	15.085	90.86	89.30	119.76	2449.8	1
#4	-65.5	-41.1	13.904	13.809	14.953	90.08	90.15	121.23	2454.9	1
#5	-65.5	-40.8	13.707	13.668	15.097	89.19	90.72	119.99	2449.4	0

Table S9: AlPO-17 with 30 water molecules per unit cell

	E_{int}	$E_{int,nodisp}$	$a / \text{\AA}$	$b / \text{\AA}$	$c / \text{\AA}$	α / deg	β / deg	γ / deg	$V / \text{\AA}^3$	$N(\text{Al}^{\text{V}})$
#1	-63.9	-40.0	13.244	13.252	15.160	90.33	89.90	120.24	2298.4	1
#2	-64.0	-39.8	13.382	13.162	15.078	89.97	90.44	119.87	2303.0	1
#3	-64.2	-40.1	13.261	13.323	15.077	89.89	90.00	120.50	2295.3	1
#4	-63.8	-38.9	13.179	13.260	15.099	89.79	90.37	119.76	2290.5	0
#5	-63.8	-39.4	13.272	13.309	15.130	90.03	89.75	120.74	2296.9	0

Table S10: AlPO-AFX with 50 water molecules per unit cell

	E_{int}	$E_{int,nodisp}$	$a / \text{\AA}$	$b / \text{\AA}$	$c / \text{\AA}$	α / deg	β / deg	γ / deg	$V / \text{\AA}^3$	$N(\text{Al}^{\text{V}})$
#1	-66.1	-42.0	13.726	13.670	20.078	90.28	89.68	120.15	3257.4	0
#2	-64.7	-40.4	13.638	13.688	20.110	90.46	89.48	119.69	3261.2	0
#3	-67.6	-44.0	13.671	13.687	20.034	90.01	89.73	119.94	3248.5	3
#4	-65.7	-41.6	13.776	13.684	19.963	89.87	89.88	119.95	3260.4	0
#5	-66.1	-42.3	13.770	13.700	19.982	89.62	89.99	120.04	3263.0	1

Table S11: *AlPO-GIS with 32 water molecules per unit cell*

	E_{int}	$E_{int,nodisp}$	$a / \text{\AA}$	$b / \text{\AA}$	$c / \text{\AA}$	α / deg	β / deg	γ / deg	$V / \text{\AA}^3$	$N(\text{Al}^V)$
#1	-65.3	-37.4	14.171	14.148	9.918	89.75	91.30	90.20	1988.0	5*
#2	-66.1	-38.0	14.233	13.950	10.012	90.09	90.44	90.11	1987.9	4
#3	-64.6	-36.2	14.205	14.001	10.005	89.44	89.68	90.60	1989.5	2
#4	-64.6	-36.5	14.119	14.017	10.096	90.21	90.71	90.87	1997.7	2
#5	-65.3	-37.7	14.362	14.062	9.926	90.08	91.67	89.74	2003.8	4

* =including one case of six-coordinated Al

Table S12: *AlPO-18 with 25 water molecules per (primitive) unit cell*

	E_{int}	$E_{int,nodisp}$	$a / \text{\AA}$	$b / \text{\AA}$	$c / \text{\AA}$	α / deg	β / deg	γ / deg	$V / \text{\AA}^3$	$N(\text{Al}^V)$
#1	-65.4	-41.4	9.304	9.372	18.782	90.53	89.08	86.60	1634.6	0
#2	-67.7	-43.8	9.318	9.474	18.487	89.38	89.96	85.05	1625.8	2
#3	-64.8	-40.7	9.340	9.333	18.702	90.32	90.52	84.88	1623.6	0
#4	-67.0	-43.3	9.393	9.384	18.574	89.87	90.81	85.64	1632.4	1
#5	-65.2	-40.9	9.353	9.353	18.650	89.64	90.85	86.36	1627.9	0

Table S13: *AlPO-RHO with 25 water molecules per (primitive) unit cell. Cell parameters of the pseudo-cubic setting (corresponding to the conventional body-centered setting of the RHO structure) are given separately in the second part of the table.*

	E_{int}	$E_{int,nodisp}$	$a / \text{\AA}$	$b / \text{\AA}$	$c / \text{\AA}$	α / deg	β / deg	γ / deg	$V / \text{\AA}^3$	$N(\text{Al}^V)$
Primitive										
#1	-63.9	-42.2	13.024	13.016	12.910	110.60	107.98	109.21	1696.9	1
#2	-63.8	-41.8	12.885	13.010	13.135	109.29	110.06	109.17	1692.8	1
#3	-66.6	-44.7	12.647	12.914	13.099	109.57	110.09	107.73	1666.6	4*
#4	-64.2	-42.0	12.844	13.000	13.110	111.19	107.75	109.36	1686.3	2
#5	-65.7	-43.3	12.955	12.721	13.078	109.30	110.18	108.03	1676.9	2
Pseudo-cubic										
#1	-63.9	-42.2	15.248	15.083	14.758	89.33	90.03	89.29	3393.8	
#2	-63.8	-41.8	14.914	15.007	15.130	90.07	89.24	90.90	3385.6	
#3	-66.6	-44.7	14.754	15.075	15.000	89.13	87.86	90.87	3333.3	
#4	-64.2	-42.0	15.302	14.942	14.754	89.82	89.09	90.83	3372.6	
#5	-65.7	-43.3	14.899	15.087	14.929	90.67	88.30	89.14	3353.7	

* = including one case of six-coordinated Al

3) DFT-D results: SAPOs with small amounts of adsorbed water

The following table reports the interaction energies and lattice parameters of the DFT-D optimised snapshots of SAPOs with small amounts of adsorbed water (one H₂O molecule per framework proton).

E_{int} Total interaction energy per water molecule (in kJ mol⁻¹)

$E_{int,nodisp}$ Non-dispersive contribution to interaction energy per water molecule (in kJ mol⁻¹)

Table S14: DFT-D results for SAPOs with one H₂O molecule per framework proton

	E_{int}	$E_{int,nodisp}$	$a / \text{\AA}$	$b / \text{\AA}$	$c / \text{\AA}$	α / deg	β / deg	γ / deg	$V / \text{\AA}^3$
SAPO-34_O1	-93.4	-70.4	13.795	= a	15.069	90	= α	120	2483.7
SAPO-17_Si1_O3	-74.2	-57.4	13.230	15.316	= a	90	= α	120	2321.5
SAPO-17_Si2_O5	-78.1	-55.0	13.276	15.338	= a	90	= α	120	2345.1
SAPO-56_Si1_O5	-88.7	-68.4	13.830	= a	19.994	90	= α	120	3311.9
SAPO-56_Si2_O4	-97.1	-73.7	13.798	= a	20.011	90	= α	120	3299.4
SAPO-43_O12	-101.5	-77.5	14.046	13.833	10.331	90	= α	= α	2007.4
SAPO-18_Si1_O12	-97.5	-75.7	9.409	= a	18.798	90.13	= α	86.96	1661.9
SAPO-18_Si2_O11	-98.5	-75.7	9.460	= a	18.584	89.99	= α	85.31	1657.4
SAPO-18_Si3_O31	-89.2	-71.2	9.456	= a	18.716	89.73	= α	85.65	1668.7
SAPO-RHO_O11	-89.3	-68.0	13.141	= a	= a	109.47	= α	= α	1746.9

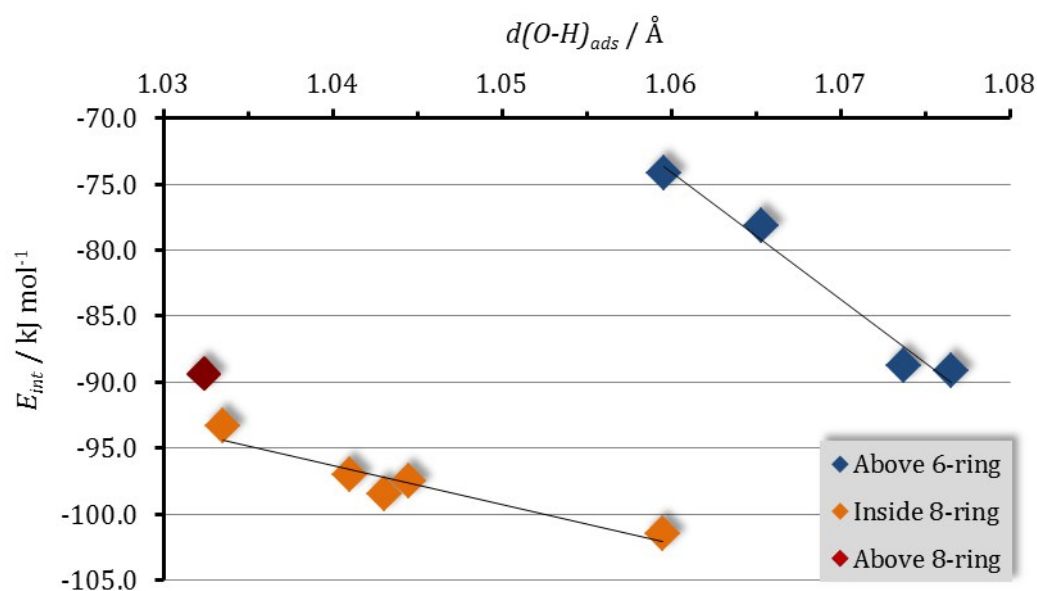


Figure S7: Plot of the interaction energy as a function of the intra-framework O-H bond length after adsorption [$d(O-H)_{ads}$]. Cases where the adsorbed water molecule is located above a six-ring, inside an eight-ring, and above an eight-ring are shown in different colours. For the former two cases, trend lines are included to guide the eye.

4) DFT-D results: SAPOs with large amounts of adsorbed water

The following tables report the interaction energies and lattice parameters of the DFT-D optimised snapshots of SAPOs with large amounts of adsorbed water (near saturation).

E_{int} Total interaction energy per water molecule (in kJ mol⁻¹)

$E_{int,nodisp}$ Non-dispersive contribution to interaction energy per water molecule (in kJ mol⁻¹)

$N(\text{Al}^V)$ Number of five-coordinated Al atoms per unit cell

Table S15: SAPO-34_01 with 40 water molecules per unit cell

	E_{int}	$E_{int,nodisp}$	$a / \text{Å}$	$b / \text{Å}$	$c / \text{Å}$	α / deg	β / deg	γ / deg	$V / \text{Å}^3$	$N(\text{Al}^V)$
#1	-71.5	-47.5	13.777	13.710	15.208	90.10	90.00	120.06	2486.1	0
#2	-72.9	-48.1	13.707	13.879	14.960	90.22	89.91	120.15	2461.1	0
#3	-72.0	-47.6	13.798	13.792	15.054	90.57	89.82	120.22	2475.3	0
#4	-73.4	-48.6	13.878	13.666	15.037	90.20	89.72	120.21	2464.4	0
#5	-73.3	-49.0	13.761	13.759	15.135	89.48	90.38	120.34	2473.2	0

Table S16: SAPO-17_Si1_03 with 30 water molecules per unit cell

	E_{int}	$E_{int,nodisp}$	$a / \text{Å}$	$b / \text{Å}$	$c / \text{Å}$	α / deg	β / deg	γ / deg	$V / \text{Å}^3$	$N(\text{Al}^V)$
#1	-69.7	-45.9	13.327	15.149	13.204	89.61	120.08	89.79	2306.6	0
#2	-70.9	-47.3	13.362	15.066	13.263	89.68	120.07	89.30	2310.3	1
#3	-69.2	-44.6	13.125	15.121	13.329	89.98	119.76	89.28	2296.1	1
#4	-68.9	-44.7	13.118	15.248	13.190	90.12	119.62	90.13	2293.5	1
#5	-69.7	-46.0	13.209	15.227	13.220	90.02	119.80	89.85	2307.3	1

Table S17: SAPO-17_Si2_05 with 30 water molecules per unit cell

	E_{int}	$E_{int,nodisp}$	$a / \text{Å}$	$b / \text{Å}$	$c / \text{Å}$	α / deg	β / deg	γ / deg	$V / \text{Å}^3$	$N(\text{Al}^V)$
#1	-70.5	-46.3	13.272	15.156	13.320	90.41	120.08	89.69	2318.5	0
#2	-72.3	-48.2	13.357	15.095	13.283	90.17	120.11	89.99	2316.8	1
#3	-72.3	-48.6	13.321	15.188	13.250	90.98	120.08	89.60	2319.4	1
#4	-73.7	-50.1	13.393	15.076	13.234	90.77	119.62	89.43	2322.7	1
#5	-71.2	-46.8	13.362	15.075	13.190	90.32	119.40	89.21	2314.6	1

Table S18: SAPO-56_Si1_05 with 50 water molecules per unit cell

	E_{int}	$E_{int,nodisp}$	$a / \text{\AA}$	$b / \text{\AA}$	$c / \text{\AA}$	α / deg	β / deg	γ / deg	$V / \text{\AA}^3$	$N(\text{Al}^V)$
#1	-69.3	-45.4	13.721	13.849	19.817	89.93	90.29	119.55	3275.8	0
#2	-70.2	-46.3	13.732	13.798	19.904	90.44	90.16	119.96	3267.3	1
#3	-69.6	-45.9	13.798	13.679	19.945	90.38	89.92	119.71	3269.5	2
#4	-69.6	-46.1	13.771	13.752	19.986	90.28	89.91	119.91	3280.5	1
#5	-70.7	-46.8	13.826	13.703	20.044	89.43	90.20	120.42	3274.7	1

Table S19: SAPO-56_Si2_04 with 50 water molecules per unit cell

	E_{int}	$E_{int,nodisp}$	$a / \text{\AA}$	$b / \text{\AA}$	$c / \text{\AA}$	α / deg	β / deg	γ / deg	$V / \text{\AA}^3$	$N(\text{Al}^V)$
#1	-70.2	-46.3	13.829	13.742	19.953	90.25	90.18	120.64	3262.6	1
#2	-68.5	-44.4	13.780	13.799	19.961	90.12	89.88	120.49	3270.6	1
#3	-68.6	-44.6	13.684	13.589	20.234	90.07	90.02	119.52	3274.0	1
#4	-69.6	-45.6	13.686	13.767	20.061	89.60	90.04	120.10	3270.1	0
#5	-69.0	-45.2	13.766	13.711	20.088	89.77	90.22	120.17	3277.8	1

Table S20: SAPO-43_012 with 32 water molecules per unit cell

	E_{int}	$E_{int,nodisp}$	$a / \text{\AA}$	$b / \text{\AA}$	$c / \text{\AA}$	α / deg	β / deg	γ / deg	$V / \text{\AA}^3$	$N(\text{Al}^V)$
#1	-69.1	-41.0	14.296	14.119	9.986	90.79	91.10	89.89	2015.2	2
#2	-70.7	-42.7	14.271	14.175	10.009	89.79	89.52	90.81	2024.3	1
#3	-70.6	-41.7	14.161	13.968	10.073	89.38	91.57	90.60	1991.5	4
#4	-73.1	-45.8	14.284	14.102	10.046	89.95	91.01	90.44	2023.3	4
#5	-72.3	-45.0	14.457	13.919	10.083	90.01	89.50	89.74	2029.0	4

Table S21: SAPO-18_Si1_012 with 25 water molecules per (primitive) unit cell

	E_{int}	$E_{int,nodisp}$	$a / \text{\AA}$	$b / \text{\AA}$	$c / \text{\AA}$	α / deg	β / deg	γ / deg	$V / \text{\AA}^3$	$N(\text{Al}^V)$
#1	-72.0	-48.2	9.407	9.471	18.640	90.57	89.78	85.53	1655.6	0
#2	-74.0	-50.3	9.448	9.429	18.532	90.30	90.19	84.81	1644.1	1
#3	-73.6	-49.5	9.412	9.382	18.707	89.76	90.27	85.55	1647.0	1
#4	-72.5	-48.3	9.434	9.327	18.763	89.04	90.34	85.99	1646.6	0
#5	-73.1	-49.2	9.410	9.333	18.730	90.13	90.69	85.45	1639.5	1

Table S22: SAPO-18_Si2_011 with 25 water molecules per (primitive) unit cell

	E_{int}	$E_{int,nodisp}$	$a / \text{\AA}$	$b / \text{\AA}$	$c / \text{\AA}$	α / deg	β / deg	γ / deg	$V / \text{\AA}^3$	$N(\text{Al}^V)$
#1	-71.0	-46.8	9.378	9.355	18.785	90.28	89.29	86.39	1644.7	0
#2	-70.8	-46.7	9.457	9.334	18.696	88.53	91.17	85.21	1643.7	0
#3	-75.0	-51.1	9.438	9.375	18.547	89.11	89.92	84.30	1632.7	1
#4	-71.4	-47.6	9.384	9.377	18.786	90.22	89.86	86.37	1649.7	0
#5	-74.5	-50.3	9.425	9.390	18.622	90.15	89.77	84.84	1641.4	0

Table S23: SAPO-18_Si3_031 with 25 water molecules per (primitive) unit cell

	E_{int}	$E_{int,nodisp}$	$a / \text{\AA}$	$b / \text{\AA}$	$c / \text{\AA}$	α / deg	β / deg	γ / deg	$V / \text{\AA}^3$	$N(\text{Al}^V)$
#1	-73.1	-49.3	9.431	9.428	18.470	91.20	89.37	86.19	1638.2	0
#2	-74.9	-51.4	9.389	9.466	18.605	89.96	89.58	86.51	1650.5	0
#3	-72.8	-49.3	9.432	9.409	18.673	89.95	90.47	85.54	1652.0	0
#4	-74.2	-50.8	9.405	9.436	18.634	90.95	89.31	87.15	1651.3	0
#5	-71.3	-47.7	9.446	9.430	18.623	89.93	90.33	86.45	1655.6	0

Table S24: SAPO-RHO_011 with 25 water molecules per (primitive) unit cell. Cell parameters of the pseudo-cubic setting (corresponding to the conventional body-centered setting of the RHO structure) are given separately in the second part of the table.

	E_{int}	$E_{int,nodisp}$	$a / \text{\AA}$	$b / \text{\AA}$	$c / \text{\AA}$	α / deg	β / deg	γ / deg	$V / \text{\AA}^3$	$N(\text{Al}^V)$
Primitive										
#1	-69.4	-47.8	13.146	13.089	13.102	111.83	107.43	109.94	1716.5	0
#2	-70.4	-48.7	13.145	12.972	12.866	107.37	109.43	111.04	1699.3	2
#3	-69.9	-47.6	12.985	13.020	13.080	110.20	109.44	108.73	1703.2	0
#4	-71.7	-49.9	13.076	12.893	13.180	109.41	109.69	109.39	1708.7	1
#5	-72.0	-50.3	13.122	13.130	12.937	109.95	109.07	110.04	1702.1	1
Pseudo-cubic										
#1	-69.4	-47.8	15.058	14.679	15.533	90.60	90.30	90.70	3432.0	
#2	-70.4	-48.7	14.787	15.301	15.026	90.45	88.59	89.76	3398.6	
#3	-69.9	-47.6	15.151	14.934	15.056	89.62	90.25	90.02	3406.5	
#4	-71.7	-49.9	15.009	15.066	15.118	89.20	89.89	91.09	3417.5	
#5	-72.0	-50.3	15.051	14.962	15.121	91.29	90.06	90.01	3404.3	

References

- 1 M. Fischer, *Phys. Chem. Chem. Phys.*, 2015, **17**, 25260–25271.
- 2 B. Zibrowius and U. Lohse, *Solid State Nucl. Magn. Reson.*, 1992, **1**, 137–148.